

Supporting Information

Conversion of multilayer graphene into continuous ultrathin sp^3 -bonded carbon films on metal surfaces

Dorj Odkhuu¹, Dongbin Shin², Rodney S. Ruoff³, and Noejung Park^{1,2}

¹Interdisciplinary School of Green Energy and Low Dimensional Carbon Materials Center,

²Department of Physics, Ulsan National Institute of Science and Technology (UNIST), Ulsan 689–798, Korea

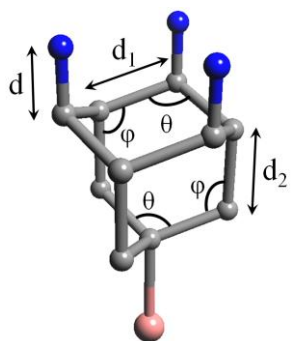
³Department of Mechanical Engineering and the Materials Science and Engineering Program, The University of Texas, Austin, Texas 78712

Correspondence to: noejung@unist.ac.kr

Supplementary Information includes:

– Table S1	page S2
– Table S2	page S3
– Figure S1	page S4
– Figure S2	page S5
– Figure S3	page S6
– Figure S4	page S7
– Discussion of Fig. 4a (from the main text)	page S8
– Computational details	page S9
– References	page S10

Table S1 | Structural properties of hydrogenated (H-ted sp^3 -C/Co) and fluorinated (F-ted sp^3 -C/Co) two-layer sp^3 carbon films on Co(0001). The corresponding results for pristine graphite and diamond structures are provided for comparison. $d_1(\text{C}-\text{C})$ and $d_2(\text{C}-\text{C})$ refer to the intralayer and interlayer C–C bonds, respectively. θ represents the C–C–C angle within the layer, and φ indicates the tetrahedral angle formed with the interlayer C–C bond. A schematic is shown below. Distances are given in Å and angles in degrees. $d(\text{A}-\text{C})$ is the bond length between the C atom in the top layer and adsorbate (H or F). Overall, the fluorinated structure revealed similar features as those for the hydrogenated structure. But the bond lengths and C–C–C bond angles of the fluorinated configurations are closer to diamond, in agreement with the previous study: fluorinated graphene has greater thermodynamic stability as compared to its hydrogenated counterpart^{S1}.



Systems	$d(\text{A}-\text{C})$	$d_1(\text{C}-\text{C})$	$d_2(\text{C}-\text{C})$	θ	φ
H-ted sp^3 -C/Co	1.11	1.52	1.58	110.2	108.5
F-ted sp^3 -C/Co	1.38	1.52	1.58	109.9	109.0
Graphite	–	1.42	3.18	120.0	90.0
Diamond	–	1.54	1.54	109.5	109.5

Table S2 | The calculated electron-phonon related features. Electronic density of states at the Fermi level $N(E_F)$ (in states $\text{Ry}^{-1}\text{cell}^{-1}$), electron-phonon coupling constant λ , logarithmic frequency average ω_{ln} (in cm^{-1}), and superconducting critical temperature T_c (in K) of the AB-stacked bilayer graphene and hydrogenated two-layer sp^3 carbon film on Cu(111) and Pt(111). The cases of B-doped sp^3 carbon film on Cu(111) are also presented with doping concentrations of 6.25% and 12.5%. To verify computational accuracy of the present work, MgB_2 (the well-known phonon-mediated superconductor) was also calculated, and the results are in reasonable agreement with previous studies^{S2,S3}.

Systems	$N(E_F)$	λ	ω_{ln}	T_c
Graphenes/Cu	4.9	0.15	316	0.00
$\text{sp}^3\text{-C/Cu}$	6.9	0.25	286	0.01
6.25% $\text{sp}^3\text{-C/Cu}$	9.1	0.33	527	0.52
12.5% $\text{sp}^3\text{-C/Cu}$	12.0	0.81	157	7.55
$\text{sp}^3\text{-C/Pt}$	10.6	0.45	257	1.90
MgB_2	4.7	0.92	598	32.5

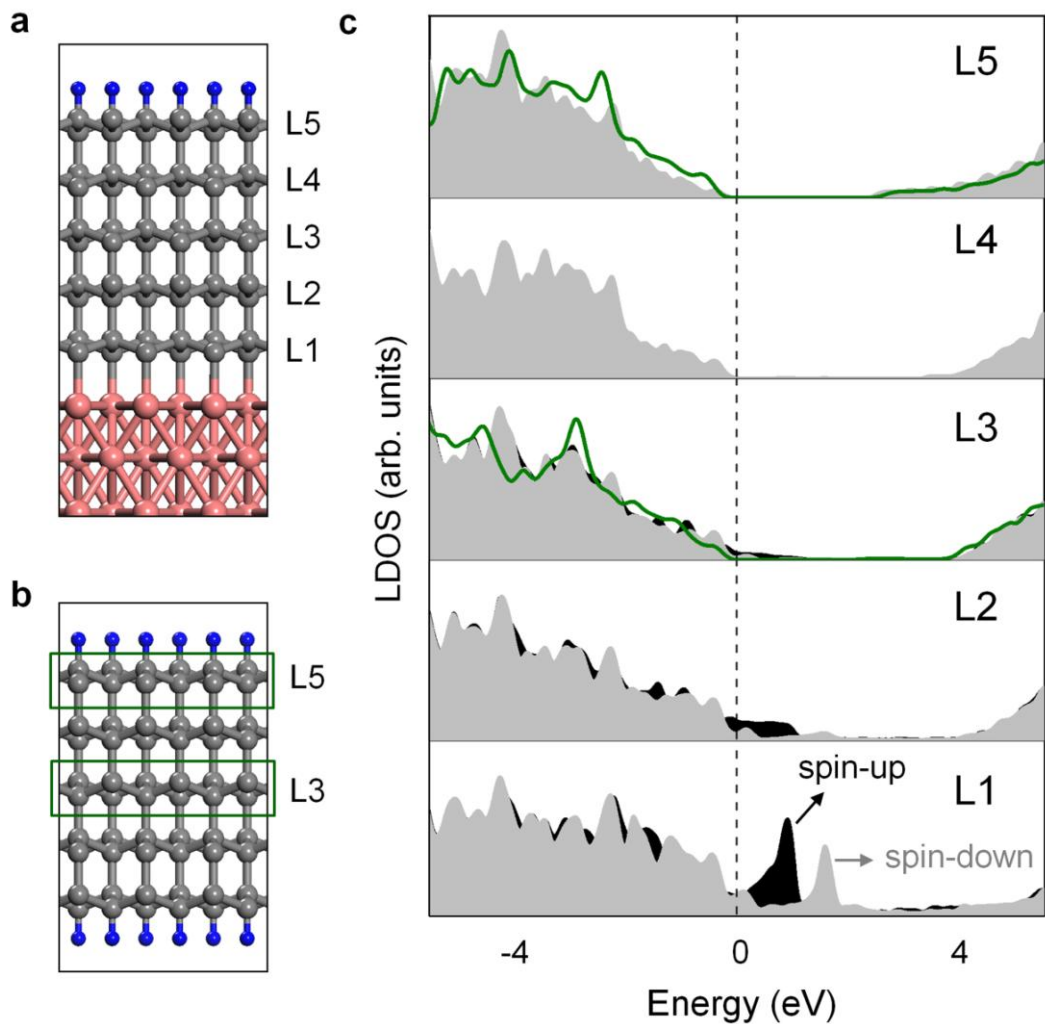


Figure S1 | (a) Atomic structures of the five-layer sp^3 carbon films on Co(0001) and (b) without Co substrate and thus with hydrogenation on both top and bottom surfaces. Blue, gray, and pink balls represent hydrogen, carbon, and cobalt atoms, respectively. (c) The density of states (DOS) for majority (dark shaded) and minority spin states (light shaded) projected onto each carbon layer. For comparison, the corresponding DOS of the center and surface layers (denoted by the green box in b) for the hydrogenated carbon films without metal substrate are plotted in green lines in the L3 and L5 panels of c. The vertical dashed line at energy zero indicates the Fermi level. In the upper layers (L4 and L5), the DOS reveal an obvious band gap that corresponds to that of diamond.

Hydrogen coverage-dependent phase transition

Angus and Hayman^{S4} related the ratio between the number of sp^3 and sp^2 bonds, $N(sp^3)/N(sp^2)$ to the H surface coverage of the ‘diamond-like hydrocarbons’ ($a-C:H$ with high sp^3 content). They developed an empirical formula based on their experimental survey: $N(sp^3)/N(sp^2) = (6X_H - 1)/(8 - 13X_H)$, where X_H is the atomic fraction of hydrogen. According to this formula, perfect sp^2 and sp^3 networks could be obtained for the hydrogen atomic fractions of 1/6 and 8/13, respectively. In the present work, we consider hydrogen adsorption only onto the outer surface and thus, Angus and Hayman’s formula cannot be directly applied. However, the coverage of $x = 1/3$ in our case (C_2H_x) can be considered similar as the coverage of $H/C = 1/6$ for $a-C:H$ because of the stabilization at the interface with the metal surface states. Figure 4a in the main text shows a ‘cross-over’ region at an H coverage of 1/3 that coincides with the transition between the covalently bonded interlayer distances ($\sim 1.64 \text{ \AA}$) and vdW-interacting interlayer distances ($\sim 3.12 \text{ \AA}$). A similar coverage-dependent structural change from sp^2 to sp^3 has also been demonstrated experimentally with single-layer graphenes on a Cu surface^{S5}.

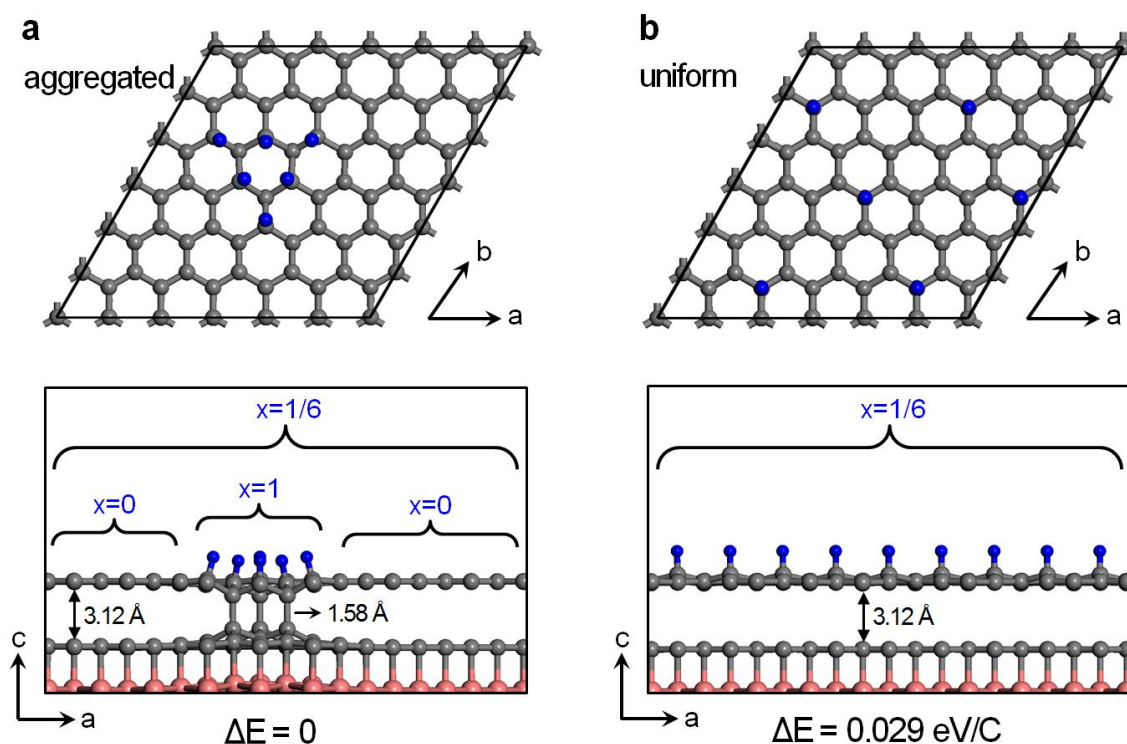


Figure S2 | (a,b) Top and side views of the optimized atomic structures of the partially hydrogenated graphene bilayer on Co(0001) surface with the hydrogen coverage of $x=1/6$ (six hydrogen atoms on 6×6 graphene supercell (72 atoms within graphene layer)). In **a**, the hydrogen adsorbates are aggregated in a region, whereas in **b** the hydrogen adatoms are uniformly distributed with similar distances from each other. Both **a** and **b** have the same overall hydrogen concentration, but **a** consists of highly concentrated region ($x=1$) and empty region ($x=0$). Atomic symbols are the same as used in Fig. S1. For simplicity, only the interface Co layer is shown. The energy difference ΔE shown at the bottom of side views are given in unit of eV per carbon atom.

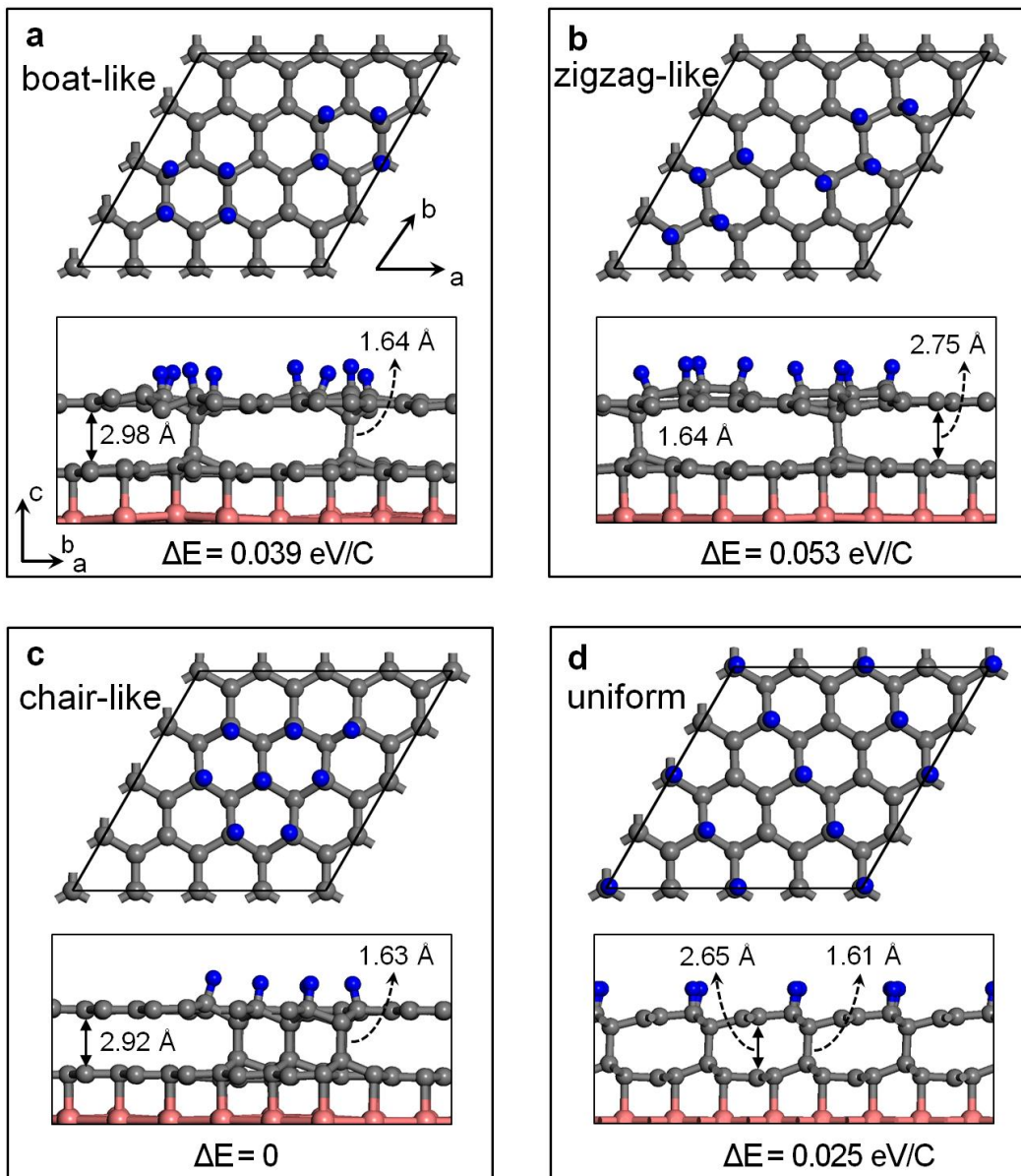


Figure S3 | (a–d) Various hydrogen adsorption configurations with the hydrogen coverage of $x=1/2$ (eight hydrogen atoms on the 4×4 graphene surface). Atomic symbols are the same as used in Fig. S2.

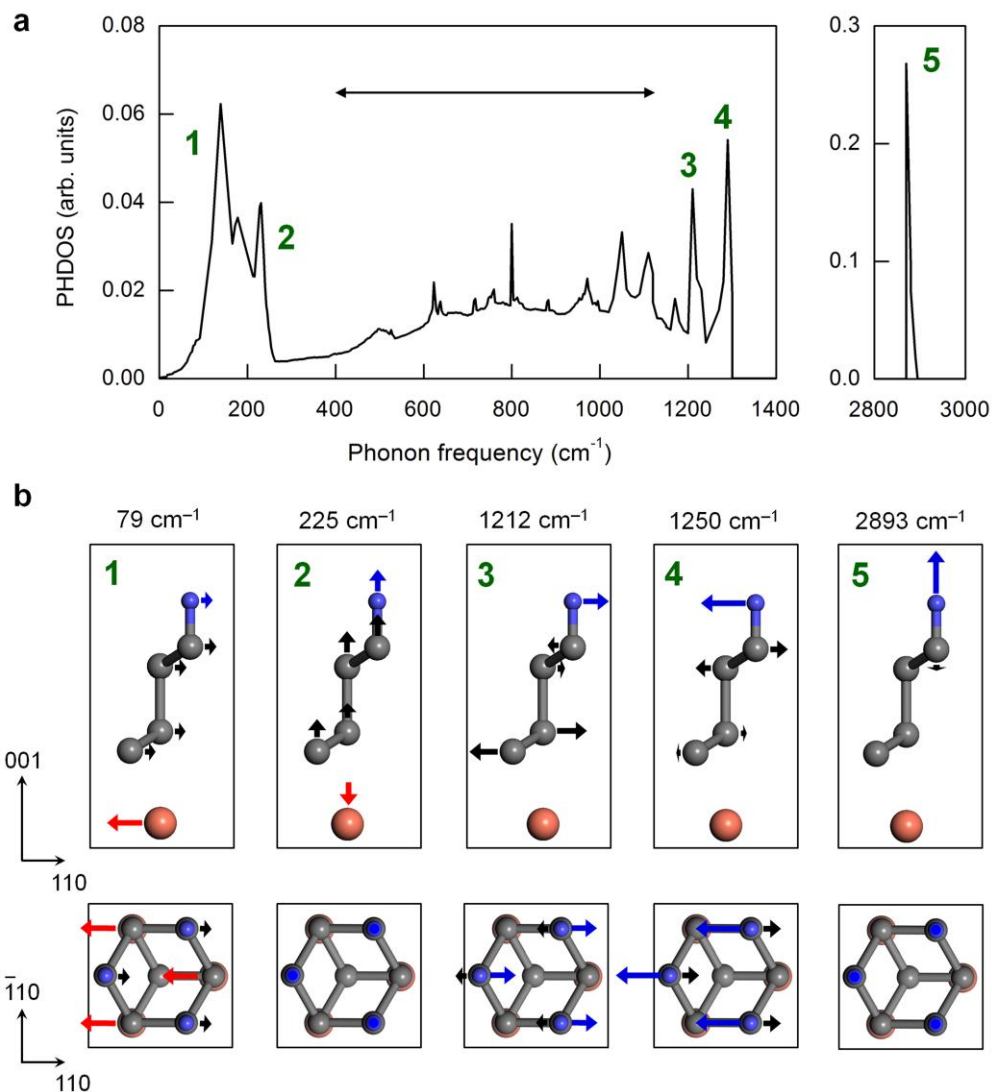


Figure S4 | (a) Phonon density of states (PHDOS) of two-layer sp^3 carbon film on Cu(111) surface. (b) The side- and top-views of the ball and stick schematics of optical phonon modes at Γ that correspond to the peaks in PHDOS. Atomic symbols follow the same convention used in Fig. S1. The low frequency region is characterized by the C–Cu vibration modes; the in-plane shearing motion (indicated by ‘1’) and the out-of-plane stretching motion (indicated by ‘2’). The high-frequency peaks denoted by ‘3’ and ‘4’ correspond to the shearing motions between C and H layers, as discussed in a previous study on graphene^{S7}. The isolated high frequency mode (2893 cm^{-1}) originates from the C–H bond stretching out of the plane, and dispersive medium-frequency region (indicated by the horizontal arrow in a) is largely contributed by the vibrations of C–C bonds.

Computational details for the supercell geometry and k-point sampling

Our model geometries consist of metal slabs with graphene overlayers. The supercell contained a large vacuum region of 15 Å along the perpendicular direction. An in-plane lattice constant of the supercell was adopted as the experimental lattice constants of metallic substrates: 2.50 Å for Co (0001), 2.49 Å for Ni (111), and 2.55 Å for Cu (111) that are well matched to the honeycomb lattice of graphene (2.46 Å), as stated in the main text. We used the 2×2 graphene cell in the lateral 2D-lattice for the most of the presented data. To access the effect of varying density of hydrogen adsorbates, as presented in Fig. 4a, we used the 4×4 and 6×6 graphene supercells that contain 32 and 72 carbon atoms within a graphene layer. The substrate metal atoms in the lowermost two layers were fixed at their corresponding experimental values, while other atoms were fully relaxed. For carbon layers without a metal substrate, both the unit cell and atomic positions were fully relaxed until the residual forces became smaller than 10^{-5} eV/Å. A kinetic energy cutoff of 400 eV was used for the plane-wave basis. Meshes of 3×3 and 9×9 k -points, in the Monkhorst-Pack scheme, were sampled for integration over the 2D Brillouin zone (BZ) for the cases of the 4×4 and 2×2 graphene supercells, respectively. The transition state and energy barriers were investigated through the nudged elastic band method^{S6}. The formation energy is defined as,

$$E_f = \frac{E_{tot}(A/\text{graphene}/M) - E_{tot}(\text{graphene}/M) - N \times E_{tot}(A)}{N}, \quad (\text{S1})$$

where $E_{tot}(A/\text{graphene}/M)$ and $E_{tot}(\text{graphene}/M)$ are the total energies of the metal-supported graphenes with and without hydrogen (or fluorine) adatoms, and $E_{tot}(A)$ is the total energy of a hydrogen/fluorine atom in the vacuum. N is the number of adsorbed adatoms.

For phonon dispersion calculations through the density functional perturbation method, a 12×12 k -point mesh with a Gaussian smearing of 0.05 Ry and a 3×3 q mesh were used in 2D BZ in a primitive graphene unit cell (1×1). The electron-phonon coupling matrix was integrated with a 72×72 k -mesh.

References

- S1. Leenaerts, O., Peelaers, H., Hernandez-Nieves, A. D., Partoens, B. & Peeters, F. M. First-principles investigation of graphene fluoride and graphane. *Phys. Rev. B* **82**, 195436:1–6 (2010).
- S2. Boeri, L., Kortus, J. & Andersen, O. K. Three-dimensional MgB₂-type superconductivity in hole-doped diamond. *Phys. Rev. Lett.* **93**, 237002:1–4 (2004).
- S3. Nagamatsu, J., Nakagawa, N., Muranaka, T., Zenitani, Y. & Akimitsu, J. Superconductivity at 39 K in magnesium diboride. *Nature* **410**, 63–64 (2001).
- S4. Angus, J. C. & Hayman, C. C. Low-pressure, metastable growth of diamond and diamondlike phases. *Science* **241**, 913–921 (1988).
- S5. Luo, Z. Q. *et al.* Modulating the electronic structures of graphene by controllable hydrogenation. *Appl. Phys. Lett.* **97**, 233111:1–3 (2010).
- S6. Mills, G. & Jonsson, H. Quantum and thermal effects in H₂ dissociative adsorption: Evaluation of free-energy barriers in multidimensional quantum systems. *Phys. Rev. Lett.* **72**, 1124–1127 (1994).
- S7. Savini, G., Ferrari, A. C. & Giustino, F. First-principles prediction of doped graphane as a high-temperature electron-phonon superconductor. *Phys. Rev. Lett.* **105**, 037002:1–4 (2010).